Non-Destructive Testing of the Quality of Wooden Columns in Zeng Jingyi's Ancient Wooden Structures

Jing Yang,^a Shaojie Wu,^b Yingcai Fang,^a Benhuan Xu,^b and Zheng Wang ^{b,*}

This study focuses on the wooden columns of a historic residential structure to assess their integrity. Employing non-invasive computed tomography (CT) scanning, the internal integrity of these ancient wooden supports was examined. Stress wave analysis, pilot nail testing, and assessments of static bending and compressive mechanical performance were performed to validate and compare the data. The findings revealed substantial variability in the material quality across the columns' crosssections, suggesting a loss of mechanical integrity that renders them unsafe for habitation or public access. A comparison between the CT scan outcomes for the Masson's pine columns and the stress wave data from the dismantled counterparts confirmed a marked degradation in their mechanical characteristics, rendering them unfit for use. The CT scan findings align with the pilot nail test results, both accurately pinpointing the condition and precise locations of defects within the columns. The static mechanical performance tests substantiated the precision and dependability of the CT scanning, pilot nail testing, and stress wave analysis in evaluating the wooden columns' quality. This research aims to establish a scientific foundation for employing diverse non-destructive testing methods in the preservation and strengthening of traditional wooden structures, thereby safeguarding our cultural heritage.

DOI: 10.15376/biores.20.1.2276-2292

Keywords: Timber structures; Column quality assessment; Computed tomography; Stress wave analysis; Pilot nail inspection; Mechanical property evaluation

Contact information: a: Department of Landscape Architecture, Jiangsu Vocational College of Agriculture and Forestry, Jurong, 212400, China; b: College of Materials Science and Engineering, Nanjing Forestry University, Nanjing 210037, China; *Corresponding author: wangzheng63258@163.com

INTRODUCTION

Chinese timber architecture boasts a rich and illustrious heritage, which is integral to the tapestry of Chinese civilization. A plethora of renowned historical and contemporary regional wooden structures grace various domains, including residential, religious, garden, and bridge construction, and these are lauded for their low-carbon footprint and ecofriendly attributes (Lao *et al.* 2022). Despite these merits, wood, being a natural material, is prone to inherent imperfections such as knots and cracks, as well as processing and environmental-induced defects (Cheng 1985), which can diminish the structural integrity and pose safety risks. The preservation of these architectural relics mandates regular inspections and assessments (Wang *et al.* 2023). Non-destructive testing (NDT) is ideally suited for on-site evaluation of such structures, offering a blend of non-invasiveness, speed, portability, and versatility. Current NDT methods for wooden components encompass stress wave, vibration, ultrasonic, resistivity, nail, radiographic, optical examinations, and finite element model analysis, surpassing the imprecision of traditional visual inspections

(Shang 2008; Wang *et al.* 2015; Niu 2023; Wang and Ghanem 2023). These techniques facilitate a comprehensive qualitative and quantitative assessment of wood defects and damage, thereby bolstering the restoration and conservation efforts of ancient timber structures.

Significant advancements have been realized in the realm of non-destructive testing and evaluation of timber structures, leveraging techniques such as stress wave detection, nail detection methods, tomographic scanning, and probability analysis (Lee 1965; Cown 1978; Wang et al. 2001; Zhang et al. 2007; Huang et al. 2010; Conde et al. 2014; Dai and Chang 2014; Wang and Ghanem 2022; Yu et al. 2023a). In a pioneering study, Hoyle and Perlin (1978) applied stress wave non-destructive testing to the glued arched beams of Douglas fir, which are critical load-bearing elements in a gymnasium in Idaho, USA. Their findings indicated that the stress wave propagation times in these glued beams were considerably longer than those in intact Douglas fir, marking a pivotal moment in the detection of wood decay. Wang et al. (2000) employed stress wave technology to assess wooden boards, revealing that defective boards exhibited longer stress wave propagation times compared to sound ones. This methodological approach provided a clear diagnostic tool for identifying wood defects by comparing propagation time differences. Divos et al. (2002) expanded the application of stress wave technology to evaluate the wooden ceiling components of the Baroque Papa Palace in Hungary. This work demonstrated that stress wave technology could accurately predict the bending strength of individual wooden elements, underscoring its utility as a communication bridge between wood scientists and construction engineers. Further research by An et al. (2008) utilized stress wave and impedance instrument technologies to map the decay distribution within the wooden columns of the Shanhaiguan Sea Temple in China. Their findings highlighted the impedance curve's ability to directly identify internal decay, although it noted the limitation of providing only a one-dimensional perspective of the decay, thus lacking a comprehensive three-dimensional understanding. Li et al. (2009) introduced a threedimensional stress wave tomography scanner and a resistance meter to assess nanmu wooden columns. This combined approach allowed for rapid acquisition of defect area data and precise determination of defect locations and severities, offering a robust method for evaluating the material condition of wooden components. Zhang et al. (2019) took nondestructive testing a step further by using a stress wave microsecond meter and an impedance meter to evaluate wooden components in ancient buildings in Guizhou. This methodology successfully determined various indicators, including dynamic elastic modulus, modulus residual rate, and residual strength, effectively diagnosing decay and insect infestation in ancient timbers. Most recently, Zhang et al. (2021) conducted nondestructive testing on wooden columns in the Forbidden City using tomography and microdrill impedance methods. They evaluated column defects and established decay distribution patterns, contributing valuable insights into the structural health of these historical timbers.

While singular testing methods have yielded valuable results, the veracity of these findings is best reinforced through a multi-modal approach. This comprehensive strategy is essential for enhancing the quality inspection and maintenance protocols of traditional wooden structures. Probabilistic methods have been used to study mechanical properties of materials (Wang and Ghanem 2021, 2023; Yu *et al.* 2023b). The ancient wooden structures of Zeng Jingyi in Nanjing, a renowned cultural heritage site established in 1864, serve as a case study for this paper. By integrating dynamic non-destructive testing methods—such as tomography, nail method, and stress wave method—with static

mechanical property assessments, this study includes an exhaustive evaluation of the building's wooden columns. The analysis identifies the origins of their defects, assesses the feasibility of column replacement, and recommends key restoration and reinforcement measures, thereby underscoring the practical engineering value of the approach. This comprehensive evaluation ultimately enhances structural integrity and extends the lifespan of the infrastructure.

EXPERIMENTAL

Stress Wave Tomography Test of the Wooden Column Structure

The layout and preservation of Zeng Jingyi's ancient wooden structures

Zeng Jingyi's ancient wooden structures are located in Hehuatang, Nanjing, Jiangsu Province. It was built in 1864. The ancient wooden structures are a combination of a temple and a residence, with clear functional divisions, solemn and elegant shape, and extremely high artistic value, as shown in Fig. 1.

This ancient wooden building complex faces south and has the existing front hall, front east-west corridors, east-west buildings, back east-west corridors, back building and east room. The protection area is 746 m². The front hall has a hard mountain roof and a raised beam wooden structure. The east-west buildings are located on the left and right of the front hall, two floors, and a through-beam wooden structure. The front east-west corridors extend forward from the east-west buildings, two floors, and a through-beam wooden structure. Due to the long-term disrepair of the building, the main wooden frame, the building roof, the building wall, and the ground have been greatly damaged and diseased. In order to ensure the continuation of the value of the cultural relics and their safe, healthy and long-term preservation, it is urgent to take necessary reinforcement and maintenance measures for the existing front hall, for instance. The wooden columns were selected for non-destructive testing. Stress wave detection and mechanical property tests were performed on the same batch of Masson pine logs.

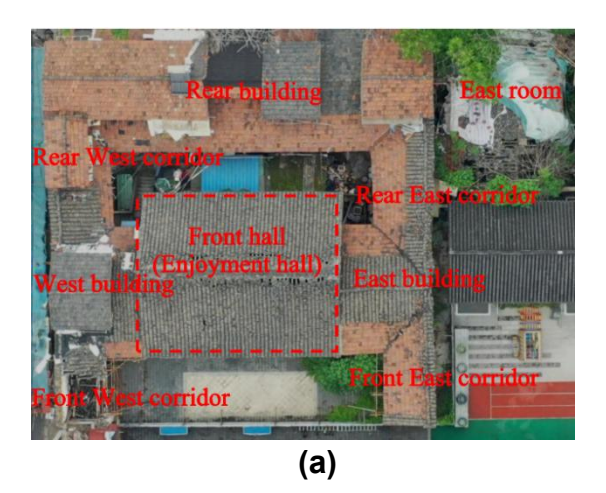




Fig. 1. (a) Floor plan of the former residence and (b) side view of the front hall

Wooden columns

The two wooden pillars are referred to as wooden pillars A and B. Each wooden pillar is 2.5 m long, with an average circumference of 0.6 m and moisture content of 19.5%

and 21.5%, respectively. The cross section of the wooden pillar is close to a perfect circle and is made of *Pinus massoniana* (Masson's pine). Its wooden column is relatively well preserved, with some cracks along the grain and serious surface corrosion defects.

Test method and principle

The stress wave tomography method was used. The stress wave imaging method is based on several assumptions to simplify the analysis and make testing more feasible. It assumes that the properties of the wood are generally uniform across different areas, or at least consistent on a macroscopic scale, in order to avoid considering small variations. Due to the anisotropic nature of wood, it is assumed that the primary direction of the wood significantly affects the propagation of the stress wave. Another assumption is that decay or defects in the wood slow down the wave speed because these areas alter the density and elasticity, which in turn affect the wave speed and are reflected as different material characteristics in the imaging. Finally, it is assumed that the propagation speed of the stress wave is related to the health of the wood, with slower wave speeds typically indicating decay or defects, and faster wave speeds suggesting healthier wood. These assumptions allow the stress wave imaging method to effectively detect internal defects in wood.

The test instrument is a PICUS acoustic tomography scanner, made in Germany, which mainly includes the main control device, sensor harness, electronic wireless hammer, rubber hammer, tape measure, nails, computer and PICUS 3 supporting program Q74STD. The accuracy of the sensor is 1 m/s.

After the wooden columns are connected with a circle of nails, the magnetic nail is hit by an electronic radio hammer, so that its sensor receives the transmitted stress wave signal, which is then transmitted to the main control device, and the material conditions in each area marked with different colors on the log fault are obtained to generate a fault color map. Finally, the wave velocity data was processed by PICUS 3 software.

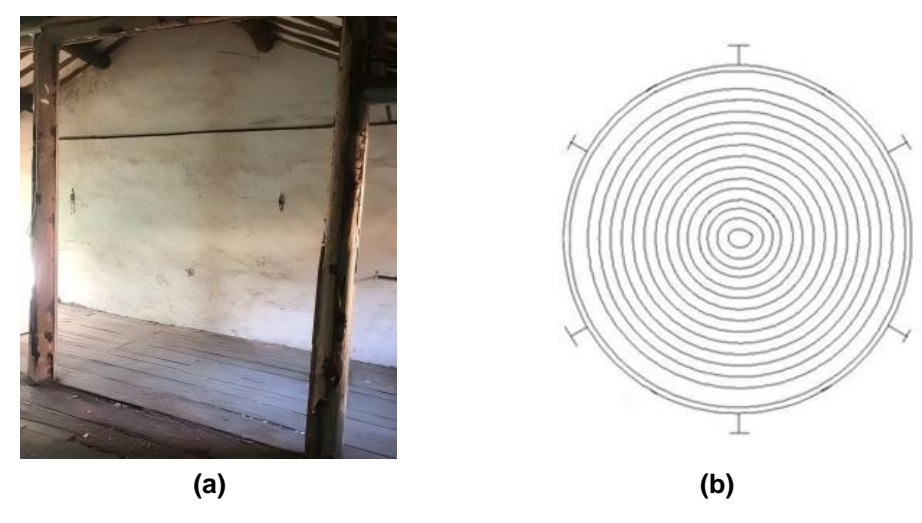


Fig. 2. (a) The wooden columns and (b) measurement point layout

The wooden columns were nailed and numbered. Specifically, wooden columns A and B were connected using six nails, as illustrated in Figs. 2(a) and 2(b). The two columns were labeled accordingly, and their average circumference and height were measured. Along the longitudinal direction of each column, test sections were marked at intervals of 30 cm from the ground, resulting in a total of three test sections for each column. These

sections were numbered A-1 to A-3 for column A and B-1 to B-3 for column B. And the parameters were set by inputting the measured circumference and height of the columns into the system, followed by system calibration. The sensor harness was then attached to the nails, ensuring that sensor number 1 is positioned on the starting point nail. Subsequently, one sensor was removed, and a magnetic nail connected to an electronic radio hammer was placed on the corresponding nail. The electronic hammer was used to strike the magnetic nail, inducing vibrations. The remaining five sensors captured the resulting stress wave signals, which were transmitted to the main control device to generate corresponding bar graphs and defect distribution maps. The collected data were processed using PICUS 3 software to determine the detailed material conditions of the wooden columns.





Fig. 3. (a) Sensor deployment site and (b) piro nail test site

Wooden Columns and Testing Equipment

The measurement of the relative density of the wood column was obtained by the depth to which the steel needle at the top penetrated the surface of the wood column, in order to verify the tomography results. The test instrument was a PILODYN, the diameter of the steel needle was 2 mm, the measuring range was 0 to 20 mm, the accuracy was 0.01 g/cm³, and the penetration was 2.0 mm into the wooden column with a preset energy. When the depth of the steel needle is displayed on a scale on the surface of the instrument, it is the test value. The main steps are: first, according to the material of the wood column, the preset energy of the steel needle is determined to be 1.5 N. Finally, place the nail instrument steadily on the surface of the wooden column, press the trigger at the bottom hard, read the depth of the steel needle and record it, and repeat the current operation according to the location of the nail.

Stress Wave Test of Dismantled Timber Columns

The test objects of this study were six Masson pine logs from the same batch dismantled, numbered 1 to 6, as shown in Table 1. The transmission speed of the stress wave in the log is first obtained; the elastic modulus value is calculated based on its wave speed and the density of the Masson pine log.

Serial Number	Length (mm)	Small Head Diameter (mm)	Moisture Content (%)
1	295	10.0	26.0%
2	369	13.2	28.5%
3	204	13.2	32.0%
4	335	10.1	23.1%
5	301	10.5	22.7%
6	375	11.0	42.0%

Table 1. Properties of Pinus massoniana Logs

Note: 1 set of HM 220 stress wave detector, including: 1 stress wave detector, 1 matching force hammer and 1 sensor, with an accuracy of 0.01km/s; 1 GM 630 moisture content meter.

Based on the acoustic properties of wood, the stress wave detector uses a specific induction probe to emit and receive the vibration beam of the stress wave propagating in the wood and measures its wave velocity, thereby judging the material properties and internal damage of the wood and obtaining the elastic modulus value of the wood. First, the six dismantled wooden columns were placed on the wooden strips, numbered, and their small head diameters were measured; then the parameters such as the length of the wooden column were set; finally, the stress wave velocity test was performed to obtain the wave velocities of the six dismantled wooden columns. The test was repeated three times to obtain the average wave velocity.

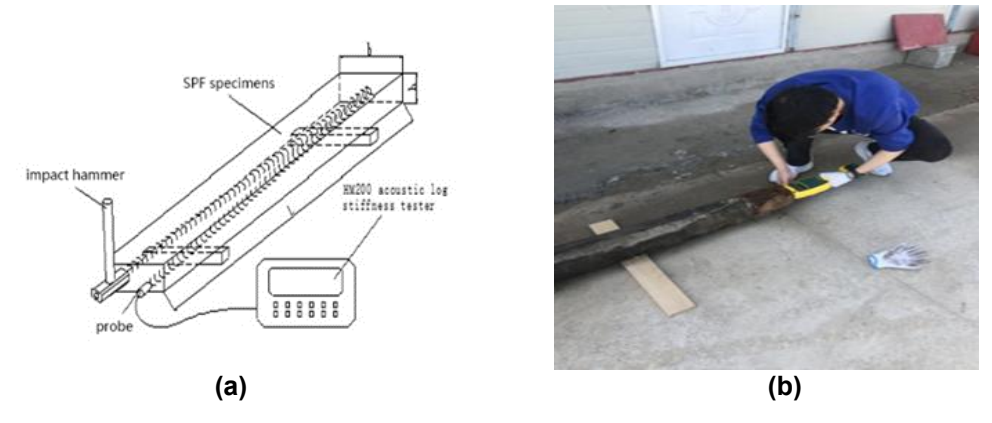


Fig. 4. (a) Stress wave test schematic and (b) stress wave detection site

Test of Wood Column Specimens

Two groups were randomly selected from six *Pinus massoniana* columns numbered 1 to 6, which underwent stress wave testing, for bending and compression performance tests. Finally, the samples numbered 4 and 6 were chosen for the tests. Through the test, the quality of the wood columns was compared and analyzed in order to make a comprehensive evaluation of the ancient wooden structures.

Moisture Content

Six test pieces with the size of $20~\text{mm} \times 20~\text{mm} \times 20~\text{mm}$ were sawn from the two wooden columns No. 4 and No. 6, numbered 4-1 to 4-6 and 6-1 to 6-6. The test instruments are an HDL intelligent electric constant temperature blast drying oven with a temperature control range of +10 to 200 °C, a Vernier caliper with an accuracy of 0.01 mm, and an ALC-210.3 electronic balance with an accuracy of 0.1 g. The moisture content and density were determined according to GB/T 1927.5 (2021).

Bending Mechanical Properties

The dismantled wooden columns No. 4 and No. 6 were sawn into 6 sawn timber specimens, all with the specifications of 300 mm \times 20 mm \times 20 mm, numbered 4-W-1 to 4-W-6 and 6-W-1 to 6-W-6. The equipment is a UTM4304 high and low temperature creep tester, and the load measurement should be accurate to 1%. The compression resistance test method is based on GB/T 1927.10 (2021). When wood is bent under force, within the proportional limit stress, the flexural modulus of wood is determined according to the relationship between load and deformation.

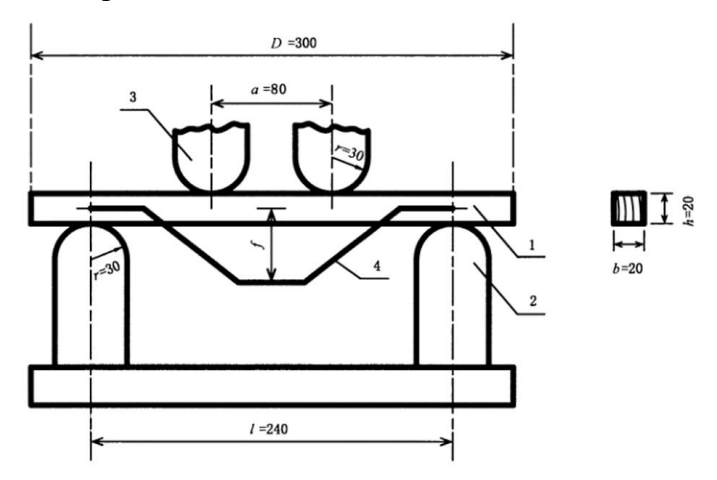


Fig. 5. Test schematic



Fig. 6. (a) Four-point flexural test and (b) specimen fracture

Compression Resistance Test

Test pieces and equipment

In the compression test along the grain, the 6 pieces cut from the dismantled wood columns No. 4 and No. 6 were all 50 mm \times 20 mm \times 20 mm, and the specimens were numbered 4-YS-1 to 4-YS-6; the sawn wood specimens from the No. 6 logs were numbered 6-SY-1 to 6-SY-6. Similarly, in the compression test across the grain, the 6 pieces cut from the dismantled wood columns No. 4 and No. 6 were all 50 mm \times 20 mm \times 20 mm, and the specimens were numbered 4-YH-1 to 4-YH-6 and 6-YH-1 to 6-YH-6. The equipment was an AG-IC 100 KN mechanical universal testing machine, and the indication error of the testing machine was \leq 1%.

Test methods and principles

This test is based on GB/T 1927 (2022). Pressure was applied along the grain of the wood at a uniform speed until it is destroyed to determine the compressive strength along the grain. To determine the compressive strength across the grain, the procedure is to load the entire surface or partial surface of the specimen in the radial or chord direction, determine the proportional limit load from the load-deformation curve of the transverse compression test, and calculate the proportional limit strength of transverse compression. To determine the transverse compression elastic modulus, the ratio of stress to strain within the proportional limit stress was calculated.

RESULTS AND DISCUSSION

Tomography Test Results and Analysis

In Fig. 7, the color of the black line between measuring points 1 and 2 is lighter than that of the other three groups, indicating that the stress wave velocity corresponding to this group of points is lower, that is, the material between the measuring points is poorer.

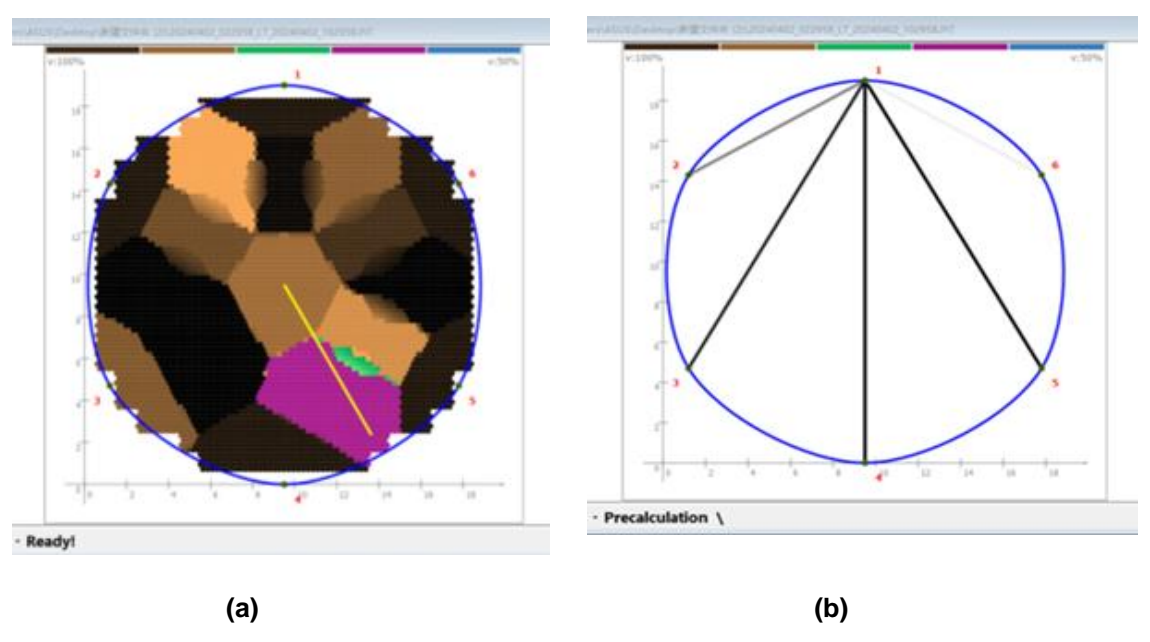


Fig. 7. (a) Tomography of section A-1 and (b) signal receiving line diagram of measurement point 1

 Table 2. Velocity Distribution Table of Section A-1 Measurement Point

Measuring Point Number	1	2	3	4	5	6
1	0	430	835	971	987	18
2	802	0	676	2468	888	680
3	418	872	0	176	277	156
4	1100	2217	542	0	482	774
5	739	963	256	507	0	449
6	436	751	845	928	29	0

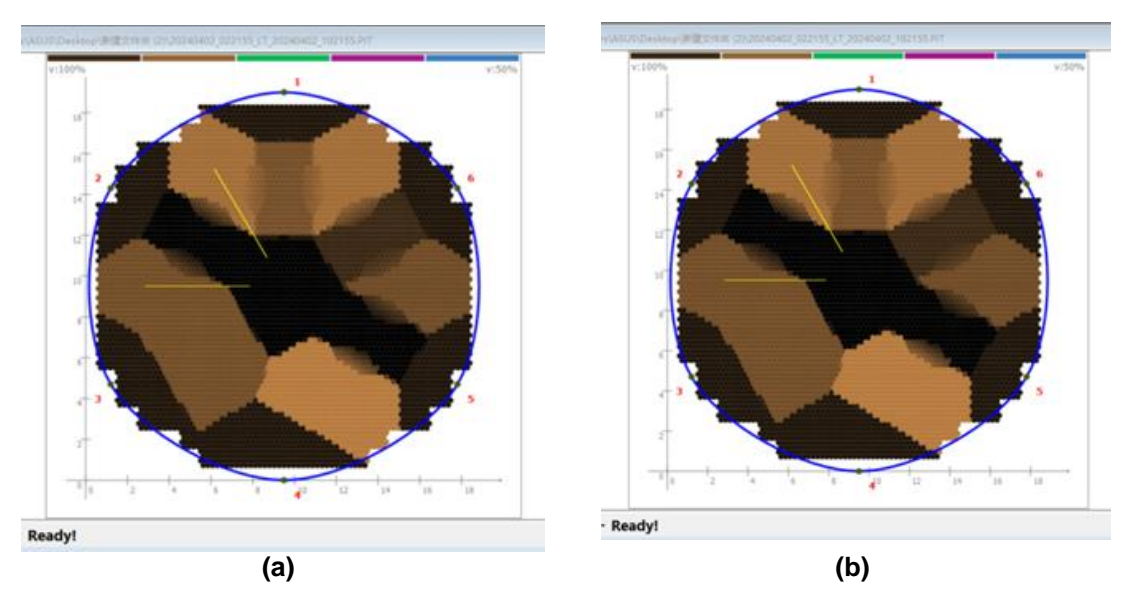


Fig. 8. (a) Section A-2 tomograph and (b) section A-3 tomograph

Table 3. Velocity Distribution Table of Section A-2 Measurement Point

Measuring Point Number	1	2	3	4	5	6
1	0	476	876	1031	975	427
2	279	0	571	896	991	824
3	1111	144	0	530	872	915
4	1151	1087	154	0	530	886
5	884	1076	1030	46	0	499
6	453	852	998	977	478	0

Table 4. Velocity Distribution Table of Section A-3 Measurement Point

Measuring Point Number	1	2	3	4	5	6
1	0	454	888	1101	1015	511
2	37	0	489	930	1104	1037
3	841	320	0	547	904	870
4	965	1233	499	0	573	836
5	869	1437	234	610	0	505
6	529	957	1144	801	668	0

Figure 9 shows the sensor signal receiving line diagram of measuring point 4 of wooden column B-1. The black line color of measuring points 4 to 5 was lighter than that of the other three groups, which indicates that the stress wave velocity between these points was lower, meaning that the material between the measuring points was poor.

The center of the tomographic image of the wooden column was mainly brown-black, and some edges were purple or green. At the same time, according to the sound velocity distribution table of the test points of the two, each sensor of the six sections of the wooden column showed multiple values with large steep amplitudes, which are represented by red, indicating that the material of the wooden column had obviously deteriorated. At the same time, the maximum stress wave velocity and the minimum stress wave velocity of the wooden column were very different. The mechanical properties of the wooden column had been seriously lost. If it is not repaired, it will be dangerous and not suitable for visiting.

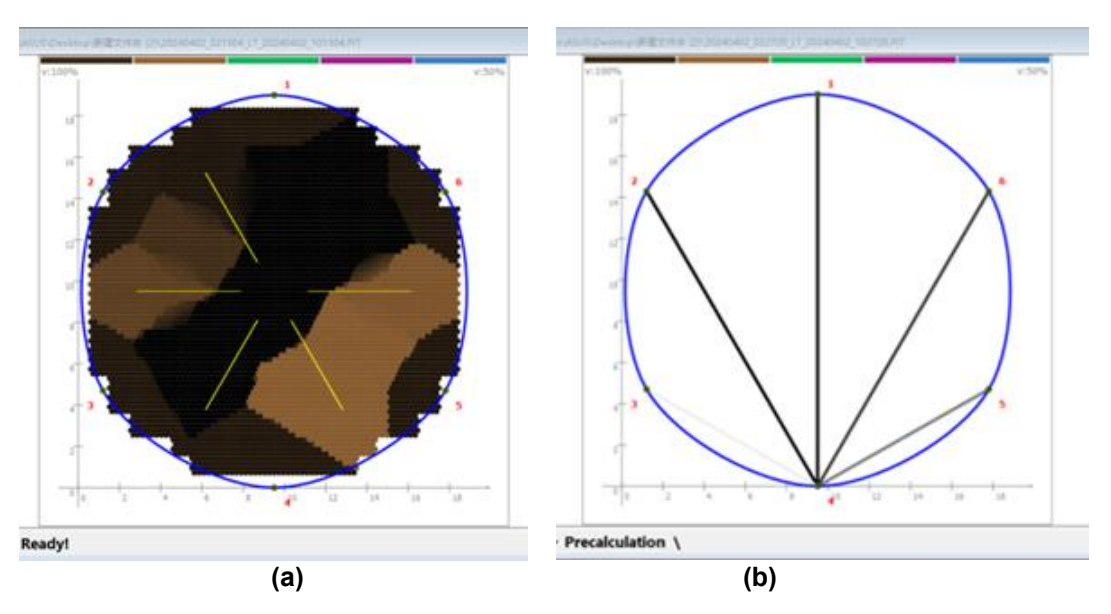


Fig. 9. (a) Section B-1 tomograph and (b) signal receiving line diagram of measurement point 4

Measuring Point Number	1	2	3	4	5	6
1	0	553	890	999	180	578
2	609	0	542	923	1214	1087
3	889	520	0	399	804	972
4	1042	1030	411	0	470	865

Table 5. Velocity Distribution Table of Section B-1 Measurement Point

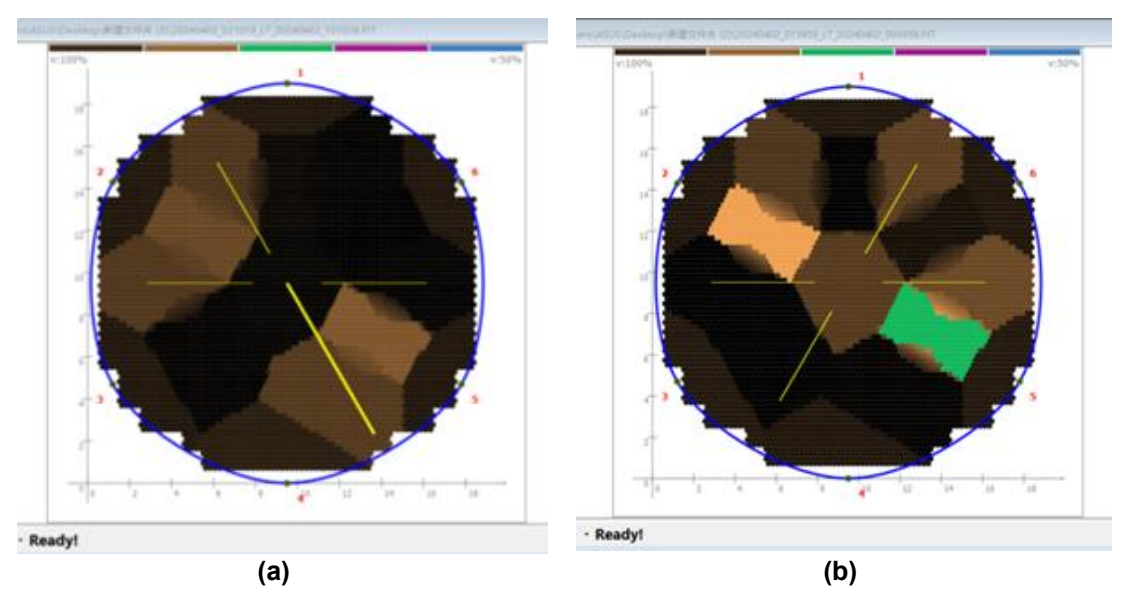


Fig. 10. (a) Section B- 2 tomograph and (b) section B-3 tomograph

Measuring Point Number	1	2	3	4	5	6
1	0	550	910	1004	1007	509
2	545	0	533	956	1638	1046
3	845	507	0	36	926	984
4	1037	1043	24	0	514	895
5	1103	529	1044	507	0	541
6	511	972	970	806	486	0

Table 6. Velocity Distribution Table of Section B-2 Measurement Point

Table 7. Velocity Distribution Table of Section B-3 Measurement Point

Measuring Point Number	1	2	3	4	5	6
1	0	576	895	1000	865	45
2	450	0	499	1004	97	875
3	823	532	0	258	989	974
4	907	1127	245	0	509	902
5	885	107	893	492	0	519
6	39	1068	1049	869	494	0

Stress Wave Method Test Results and Analysis

The results of longitudinal stress wave testing on the six Masson pine column specimens removed are shown in Tables 8 and 9.

Table 8. Analysis of Stress Wave Test Results

Serial Number	Wave Speed 1 (km/s)	Wave Speed 2 (km/s)	Wave Speed 3 (km/s)	Average Wave Speed (km/s)	Elastic Modulus (MPa)
1	5.14	5.17	5.14	5.15	6895
2	5.21	5.21	5.21	5.21	7057
3	2.41	2.43	2.42	2.43	1535
4	5.16	5.16	5.16	5.16	6922
5	4.97	4.98	4.99	4.98	6448
6	4.99	5.01	5.03	5.01	6526

As shown in Table 8, because the logs came from the same batch of Masson's pine, the stress wave transmission wave velocity was roughly the same, that is, the longitudinal elastic modulus was not much different. However, the Masson's pine log numbered 3 was quite different from other Masson's pine logs. This is because there was a 1400 mm \times 15 mm crack and a 120 mm \times 20 mm mortise and tenon joint on the surface of the wooden column. Obviously, the propagation characteristics of sound waves in the "gaseous" medium of the No. 3 wooden column specimen will negatively affect its wave velocity value, and the test results of No. 3 can be ignored. The average wave velocity of the remaining 5 wooden column specimens was 5.10 km/s. Its elastic modulus was 6770 MPa, and its coefficient of variation (COV) was 3.94%, which cannot meet the requirements of third-class materials.

Analysis of the Piro Nail Method

As shown in Table 9, there were some differences in the surface density of the three fault sections of the A wooden column, which was mainly determined by the actual decay of the wooden column. The deeper the decay of the wooden column, the lower the density.

However, judging from the average depth of the three fault sections, the density difference between the surfaces of wooden columns A and B was not large.

 Table 9. Test Results of Wooden Cylinders Tested by Piro Nail Method

Serial Number	Depth 1 (mm)	Depth 2 (mm)	Depth 3 (mm)	Depth 5 (mm)	Depth 6 (mm)	Average Depth (mm)
A-1	14	19	14	20	15	13.5
A-2	14	14	17	18	14	15.5
A-3	15	15	14	13	14	14.0
Mean						14.3
B-1	12	14	12	15	16	14.8
B-2	15	15	17	16	17	15.8
B-3	20	17	15	18	17	17.2
Mean						15.9

Density and Moisture Content

The average density of this batch of Masson's pine logs was measured to be 0.36 g/cm³, slightly lower than the standard density of Masson's pine of 0.383 to 0.491 g/cm³. This shows that after 160 years, the density of the wooden columns of Zeng Jingyi's ancient wooden structures in Nanjing was lower than the standard density. The average moisture content of this batch of Masson's pine logs was 12.4%, which is relatively moist.

Flexural Mechanical Properties

As shown in Table 10, the bending strength and bending elastic modulus of the test specimens starting with No. 4 and No. 6 were similar, but the results between the two were quite different. This is mainly because the 12 test specimens were taken from two different Masson's pine logs, and the bending strength and bending elastic modulus of the log No. 6 were lower, and the performance was poorer.

 Table 10. Test Results of Bending Mechanical Properties

Serial	Width	Thickness	Length	Destruction	Bending	Elastic Modulus
Number	(mm)	(mm)	(mm)	Load (N)	Strength (MPa)	(MPa)
4-W-1	19.32	19.77	292	1875	89.34	6722.76
4-W-2	20.12	19.87	297	1211	64.88	5806.74
4-W-3	20.27	20.11	282	1493	65.57	5847.80
4-W-4	20.88	19.87	285	1995	87.12	6519.19
4-W-5	19.67	19.21	296	1564	77.57	6003.79
4-W-6	20.33	19.65	289	1927	88.37	6687.00
Mean					78.81	6264.21
COV/%					16.3	10.17
6-W-1	19.95	20.11	297	1179	52.61	3889.64
6-W-2	20.65	19.51	284	1241	56.84	4331.67
6-W-3	20.20	20.07	275	1046	46.28	3428.57
6-W-4	20.57	21.07	282	1551	61.14	4314.78
6-W-5	19.79	20.63	295	1555	66.46	4790.29
6-W-6	19.58	21.05	304	1276	52.95	3739.87
Mean					56.05	4082.27
COV/%					12.06	12.01

Compressive Strength

From Table 11 and Table 12 it can be observed that the test results were consistent with the conclusions drawn from Table 10. That is, the compressive strength and compressive elastic modulus values of the specimen No. 6 in both the longitudinal and transverse directions were smaller than those of the specimen No. 4. The bending and compression resistance of the logs were far from the standard.

Table 11. Test Results of Compressive Strength along the Grain

Serial Number	Width (mm)	Thickness (mm)	Maximum Breaking Load (N)	Specimen Compression Strength (MPa)
4- YS-1	19.50	20.09	12846	32.79
4- YS-2	19.97	20.27	13512	33.78
4- YS-3	19.53	19.52	10915	28.63
4- YS-4	19.48	20.04	9840	25.21
4- YS-5	19.81	18.91	12087	32.23
4- YS-6	19.84	18.85	11806	31.57
Mean				30.70
COV/%			11.16	10.44
6- YS-1	19.35	19.89	10271	26.69
6-YS-2	19.97	19.57	11615	29.72
6-YS-3	19.96	19.41	10109	26.09
6-YS-4	20.00	19.78	9928	25.10
6-YS-5	19.78	19.13	12078	31.92
6-YS-6	20.09	20.12	10006	24.75
Mean				27.39
COV%			9.7	10.37

Table 12. Results of Transverse Compressive Strength and Transverse Compressive Elastic Modulus

Serial Number	Width (mm)	Thickness (mm)	Maximum Breaking Load (N)	Compression Strength (MPa)	Elastic Modulus (MPa)
4-YH-1	18.51	19.85	2354	6.41	533.90
4-YH-2	20.16	18.56	2785	7.44	620.26
4-YH-3	19.97	20.01	2699	6.75	562.85
4-YH-4	19.67	20.07	3104	7.86	655.22
4-YH-5	20.25	19.77	2752	6.87	572.84
4-YH-6	20.89	19.91	2960	7.12	593.06
Mean				7 .08	589.69
COV/%				7 .32	7.34
6-YH-1	19.91	19.75	2091	5.32	443.13
6-YH-2	20.06	19.06	1989	5.20	433.51
6-YH-3	19.53	20.13	1542	3.92	326.86
6-YH-4	19.85	20.35	1774	4.39	365.87
6-YH-5	17.73	20.13	1909	5.09	415.78
6-YH-6	20.31	20.19	1672	4.08	339.79
Mean				4 .67	387.49
COV/%				11.31	12.87

According to the provisions of GB 50005-2017 for the classification of pine wood, the elastic modulus of first-class wood must be greater than 8600N/mm², the elastic

modulus of second-class wood is 7400 to 8600N/mm², and the elastic modulus of third-class wood is 7000 to 7400 N/mm². The result show that the elastic modulus of the Masson's pine logs did not meet the elastic modulus requirements of third-class wood.

Test Results and Analysis of Overall Mechanical Properties of Wood Columns

Stress wave tomography showed that the center of the tomographic image of the wooden column was mainly brown-black, and some edges were purple or green. The brown color in the image represents that the stress wave velocity was fast and the wood material was good; while purple and green represent that the stress wave velocity was slow and the material was poor. This shows that the wooden column, which has been around for 160 years, has been basically preserved intact despite more or less defects such as decay and cracks inside.

The sound velocity distribution results of the measuring points showed that each sensor of the three sections of the wooden columns had multiple values with large abrupt amplitudes, which are represented by red, indicating that the material of the wooden columns had obviously deteriorated. At the same time, the maximum stress wave velocity and the minimum stress wave velocity of the wooden columns were very different, with the minimum stress wave velocity being only 18 m/s and the maximum being 2468 m/s. The mechanical properties of the wooden columns had been seriously lost. If they are not repaired, they will be dangerous and unsuitable for living or visiting.

The comparative analysis of the tomographic scan images and the Piro nail test results showed that there were areas with poor material quality at the edges of sections A-3 and B-3, and the Piro nail had the greatest penetration depth in this area. The Piro nail test results were consistent with the tomographic scan images.

Wave testing of the 6 dismantled wooden columns showed that the longitudinal elastic modulus values of the wooden column specimens can be calculated. Among them, only the elastic modulus of the No. 3 wooden column specimen was only 1537 MPa, while the elastic modulus values of the other 5 wooden column specimens were not much different. However, the elastic modulus values of the 6 wooden columns did not meet the requirements of the third-class materials.

Through the random selection of No. 4 and No. 6 wood column specimens from the 6 dismantled wood columns, the density, moisture content, bending and compressive physical properties tests were carried out, and the elastic modulus values were basically consistent with the longitudinal stress wave test results. The bending and compressive properties of wood column logs were far below the existing standards. The average elastic modulus of this wood column was 5173 MPa, which does not meet the existing third-class material elastic modulus standard requirements. According to "Wood Science", the average compressive strength of Chinese wood along the grain is 45 MPa, and the compressive strength along the grain is generally 5 to 10 times the compressive strength across the grain. The compressive strengths shown in Table 11 and Table 12 are lower than this value, so the performance of the Masson's pine material can be regarded as poor.

CONCLUSIONS

- 1. Examination of the 160-year-old wooden columns from Zeng Jingyi's ancient wooden structures in Nanjing revealed extensive surface damage, characterized by visible signs of decay and cracking. Tomographic imaging depicted a brown-black core with purple-green edges, indicating a stark material quality disparity. The stress wave velocities varied dramatically, from a minimum of 18 m/s to a maximum of 2468 m/s, underscoring a significant loss in mechanical properties. This divergence suggests that the columns had compromised structural integrity, posing a risk if left unrepaired, and rendering them unsafe for occupancy or public access.
- 2. Building of the former residence and stress wave tests on the dismantled Masson's pine wooden columns of the former residence showed that the wood defects of the Masson pine wooden columns were relatively serious, their mechanical properties had changed significantly, and they are now unusable.
- 3. The Piro nail method corroborated the tomographic images, demonstrating the PICUS 3 stress wave tomography's non-destructive testing technology's ability to accurately pinpoint the condition and precise location of defects within the wooden columns.
- 4. The precision and reliability of non-destructive testing methods, including tomography, nail testing, and stress wave testing, were validated for assessing the quality of wooden columns. The results indicate that the Masson's pine columns' resistance to bending and compression falls below the standards for third-class materials, highlighting the necessity for intervention to restore their load-bearing capabilities.

ACKNOWLEDGMENTS

This research was supported by 2024 Jiangsu Vocational College of Agriculture and Forestry Fund Cultivation Science and Technology Project (2024ki31).

Conflicts of Interest

The authors declare that they have no known competing financial interests or personal relationships that could have appeared to influence the work reported in this paper.

REFERENCES CITED

- An, Y., Yin, Y. F., Jiang, X. M., and Zhou, Y. C. (2008). "Investigation of decay distribution of wooden columns in wooden structures using stress wave and impedance instrument technology," *Journal of Building Materials* 11(4), 457-463.
- Cheng, J.Q. (1985). Wood Science, China Forestry Publishing House, Beijing.
- Conde, M. J. M., Liñán, C. R., and De Hita, P. R. (2014). "Use of ultrasound as a nondestructive evaluation technique for sustainable interventions on wooden structures," *Building and Environment* 82, 247-257. DOI: 10.1016/j.buildenv.2014.07.022
- Cown, D. J. (1978). "Comparison of pilodyn and torsiometer methods for the rapid assessment of wood density in living trees," *New Zealand Journal of Forest Science*

- 8(3), 384-391.
- Dai, J., and Chang, L. H. (2014). "Research on nondestructive testing methods and damage repair of ancient wooden structures," *Construction Technology* 43, 55-59.
- Divos, F., Nemeth, L., Bejo, L. (2002). "Evaluation of the wooden structures of a baroque palace in Papa, Hungary," in: *Proceedings of the 11th International Symposium on Nondestructive Testing of Wood*, Sopron, Hungary.
- GB/T 1927.5 (2021). "Test methods for physical and mechanical properties of flawless small specimens of wood. Part 4: Determination of moisture content," Standardization Administration of China, Beijing, China.
- Hoyle, R. J., and Perllerin, R. F. (1978). "Stress wave inspection of a wood structure," in: *4th Nondestructive Testing of Wood Symposium*, Pullman, WA, USA, pp. 33-45.
- Huang, R. F., Wu, Y. M., and Li, H. (2010). "Analysis of the results of nail testing on the decay of old wood in ancient buildings," *Journal of Forestry Science* 46(10), 114-118. DOI: 10.11707/j.1001-7488.20101019
- Lao, W. L., Duan, X. F., Lu, B., Zhang, Z. T., and Wang, Y. (2022). "Analysis of the development path of the wood industry under the goals of carbon peak and carbon neutrality," *Wood Science and Technology* 36(1), 87-91. DOI:10.12326/j.2096-9694.2021153
- Lee, I. D. G. (1965). "Ultrasonic pulse velocity testing considered as a safety measure for timber structures," in: 2nd Nondestructive Testing of Wood Symposium, Spokane, WA, USA, pp. 185-203.
- Li, H., Liu, X. Y., and Chen, Y. S. (2009). "New technology for nondestructive testing of ancient building wooden structures," *Wood Industry* 23(2), 18-20. DOI: 10.19455/j.mcgy.2009.02.013
- Niu, Y. X. (2023). "Research on nondestructive testing methods and applications of ancient building wooden components," *Construction Science and Technology* (13), 22-25. DOI: 10.16116/j.cnki.jskj.2023.13.023
- Shang, D. J. (2008). Research on the Application of Nondestructive Testing and Evaluation Technology in the Maintenance of Ancient Building Wooden Components, Northwest Agricultural and Science University.
- Wang, Z. H., Gao, Z. Z., Wang, Y. L., Cao, Y., Wang, G. G., Liu, B., and Wang, Z. (2015). "A new dynamic testing method for elastic, shear modulus and Poisson's ratio of concrete," *Construction and Building Materials* 100, 129-135. DOI: 10.1016/j.conbuildmat.2015.09.060
- Wang, X. P., Ross, R. J., Michael, M., Barbour, R. J., John, R. E., Forsman, J. W., and McGinnis, G. D. (2001). "Nondestructive evaluation of standing trees with a stress wave method," *Wood and Fiber Science* 33(4), 522-533.
- Wang, X. P., Ross, R., Erickson, J., Forsman, J., McGinnis, G., and De Groot, R. C. (2000). Nondestructive Methods of Evaluating Quality of Wood in Preservative-treated Piles (FPL-RN-0274), U.S. Department of Agriculture, Forest Products Laboratory, Madison, WI.
- Wang, Z., and Ghanem, R. (2021). "An extended polynomial chaos expansion for PDF characterization and variation with aleatory and epistemic uncertainties," *Computer Methods in Applied Mechanics and Engineering* 382, article 113854. DOI: 10.1016/j.cma.2021.113854
- Wang, Z., and Ghanem, R. (2022). "A functional global sensitivity measure and efficient reliability sensitivity analysis with respect to statistical parameters," *Computer Methods in Applied Mechanics and Engineering* 402, article 115175. DOI:

- 10.1016/j.cma.2022.115175
- Wang, Z., and Ghanem, R. (2023). "Stochastic framework for optimal control of planetary reentry trajectories under multilevel uncertainties," *AIAA Journal* 61(8), 257-3268. DOI: 10.2514/1.J062515
- Wang, Z., Hawi, P., Masri, S., Aitharaju, V., and Ghanem, R. (2023). "Stochastic multiscale modeling for quantifying statistical and model errors with application to composite materials," *Reliability Engineering and System Safety* 235, article 109213. DOI: 10.1016/j.ress.2023.109213
- Wang, Z. H., and Ghanem, R. (2023). "Stochastic modeling and statistical calibration with model error and scarce data," *Computer Methods in Applied Mechanics and Engineering* 416, article 116339. DOI: 10.1016/j.cma.2023.116339
- Yu, T. H., and Wang, Z. H. (2023a). "Model updating of nonproportionally damped structural systems using an adapted complex sum-of-squares optimization algorithm," *Journal of Engineering Mechanics* 149(8), article 04023043. DOI: 10.1061/JENMDT.EMENG-6953
- Yu, T. H., Wang, Z. H., and Wang, J. F. (2023b). "An iterative augmented unscented kalman filter for simultaneous state-parameter-input estimation for systems with/without direct feedthrough," *Mechanical Systems and Signal Processing* 205, 110793. DOI: 10.1016/j.ymssp.2023.110793
- Zhang, D., Yu, Y. Z., Guan C., Wang, H., Zhang, H. J., and Xin, Z. B. (2021). "Nondestructive testing of defects in wooden columns of the old official Yangxin Hall," *Journal of Beijing Forestry University* 43(5), 127-139. DOI: 10.12171/j.1000-1522.20210028
- Zhang, X. F., Li, H., Liu, X. Y., Zhang, S. B., and Huang, R. F. (2007). "Application of wood resistance meter testing technology," *Wood Industry* 21(2), 41.
- Zhang, Y. X., Wang, Y., Zhang, G. J., and Guang, Z. Z. (2019). "Application of stress wave and impedance instrument technology in the detection of ancient building wooden structures," *Earthquake Resistance and Retrofitting Engineering* 41(1), 145-157. DOI: 10.16226/j.issn.1002-8412.2019.01.021

Article submitted: September 24, 2024; Peer review completed: December 8, 2025; Revised version received and accepted: January 26, 2025; Published: February 1, 2025. DOI: 10.15376/biores.20.1.2276-2292